Solid-solution-formation by MM of the Ag-70at%Cu alloy

[1,2] H. Zoz, [2] S. Morales and [2] D. Jaramillo V.
[1] Zoz GmbH, D-57482 Wenden, Germany
[2] ESIQIE, National Polytechnic Institute, Mexico City, DF 07300, Mexico

Abstract

The solid-solution-formation of the well known Ag-70Cu (at%) has been chosen to study efficiency, Fe-contamination and particle-morphology evolution in a Simoloyer CM01-2l high energy mill.
Grinding media/powder ratio was varied at constant media load of 1500g. Samples for solid-solution and for morphology-evolution were taken out at different times. The media/powder ratio was compensated by discharging the corresponding load of balls for the extracted sample.
Solid-solution-formation was obtained after 79.2, 43.2 and 18 ks for the 10:1, 20:1 and 50:1 ratio respectively. Fe-contamination was always lower than 1.0%.
Solid-solution-formation mechanism for this ductile material under MM seems to be related to the flake-formation-mechanism occurring during the collision of grinding media. Additionally, Cycle Operation has been applied which resulted in rapid flaking with quasi-disappearing ductility followed by shear-stress to break the flaky structure repeatedly.
Since a higher collision rate versus shear and friction effect is expected to cause less abrasive wear on the milling tools, the Fe-contamination was expected and found in low range.
Material's characterization is given by SEM, XRD and TEM.

1. Introduction

The aim of the present paper is a better understanding of the mechanism for the solid solution formation (SSF) by MM (Mechanical Milling) where we chose the example of Ag-70Cu (at%). We want to study efficiency in SSF, Fe-contamination and particle-morphology evolution in a Simoloyer CM01-2l high energy mill. In this work we did not use HKP (High Kinetic Processing) which would refer to a relative velocity of grinding media in the order of 9 m/s and higher but medium kinetic processing in the order of 4 m/s since we want to study the flake formation which at HKP in case of ductile metals is performed to fast.
The Ag-Cu-system is attractive to investigate SSF since it was one of the first systems studied by Mechanical Alloying (MA) and is perfectly defined by low energy milling and has perfectly been characterized [1-3]. It is a system very noble and easy to work with when a matter of comparison wants to be made. SSF is favoured because Cu and Ag belong to the same group in the periodic table. On the other hand, Ag and Cu do not form a SS in conventional melting route because of their significantly different atomic radii. Finally we can expect high deformation rates at relatively low sheer stress due to the fcc-structure of both of the materials which is expected to favour the SSF by quasi-thin-layer formation on micro-structural base.

What makes the Simoloyer interesting here, is the high (or medium) kinetic process based not on shear and friction (low kinetic processing) but mainly on the collision of grinding media at relative velocities up to 14 m/s [4-5] which first promises a high level of energy impact and second a lower level of impurities res. of contamination by the milling tools since collision is naturally less abrasive than shear and friction effects. Since it is well known that the mode of impact by the Simoloyer can lead to very thin flakes when processing ductile metals [6-8], this is exactly what we expect to need for a fast and complete SSF. This is the expected future application and this is why we did chose this system but at lowered medium kinetic for the present work.

Figure 2: collision effects in HKP (Simoloyer)

Figure 1: horizontal rotary ballmill (Simoloyer CM01-2l) with air-lock for loading, operation and unloading under vacuum and/or inert-gas.

Figure 1 shows a Simoloyer CM01-2l which is a horizontal rotary ballmill with a 2 liter chamber volume that can be placed on a table next to the process controlling computer which is operated with water cooling or heating at rotation frequencies up to 1800 rpm. Figure 2 shows a real image of a Simoloyer CM01 with a transparent chamber in operation where the effect of collision in MM is visualized and the working principle can be imagined where the rotor is the tool to transfer the kinetic energy into the grinding media and the grinding media transfers into the powder material.

2. Experimental

2.1 Ag- and Cu-powder

The detailed composition of the Ag-Cu powder-mixture that we used for the processing is given in table 1. Both of the starting materials were based on the chemical production route and therefore of high purity.

starting powder mixture for MM to achieve flake formation and SSF				
element	purity [%]	PS [µm]	comp. [at%]	comp. [wt%]
Ag	99.9	1-10	bal.	bal.
Cu	99.5	1-5	70	57.88

Table 1: Ag-Cu-starting powder mixture

Since both materials are classified as CMB-materials [9-11] due to their ductility and are known to cause problems in terms of sticking and agglomeration tendency in a mechanical milling (MM) process, we decided to use Cycle Operation [9-14] and since of that we did not use any PCA as a lubricant in the process.
MM was performed under argon-atmosphere which means a standard air-lock was used to transfer the starting powders from an argon-container into the evacuated grinding chamber which was after that flooded with argon. Detailed parameters and procedure are given in chapter 2.2.

2.2 MM-process

The laboratory-scale Simoloyer CM01-2l has been used for the MM but only at medium kinetic and this was carried out for 0.9, 1.8, 3.6, 14.4, 18.0, 36, 54, 72, 75.6, 79.2, 82.8 and 86.4 ks which refers to intervals from 15 min to 24 h. In order to investigate expected early flake formation, we took samples after 3, 5, 7, 10, 15 and 30 minutes within the first 3 reported operations (0.9, 1.8, 3.6 ks). In order not to change the powder/ball weight ratio, we extracted next to a small powder sample always the corresponding mass of grinding media in these 3 tests. All together, 18 samples have been taken in the early stage. Here we also varied the powder/ball weight ratio and used 1:10, 1:20 and 1:50.

The detailed process-parameters are given in table 2 and tables 3 and 4 give the processing-schedules for the investigation of flake-formation and SSF respectively.

process parameters of Ag-Cu-powder mixture in the Simoloyer	
milling device	Simoloyer CM01, 2.7 kW,
operating software	Maltoz 3.1
grinding unit	W01-2l (2 liter, water-cooled)
grinding media	Chromium steel, 100Cr6, 5 mm, 1.4-1.5 kg varied
PCA (lubricant)	no > Cycle Operation
starting powder	Ag-70Cu (mixture by at%)
starting powder load	varied at 30, 75 and 140 g
powder/ball weight ratio	1:10, 1:20 and 1:50 varied
atmosphere	Argon, preceding evacuation
Operation Cycle	600/150 rpm - 14/1 min (refers to 3.6 m/s)
Discharging Cycle	150/600 rpm - 4/1 min
average discharging time	10-20 min, sampling time 1 min
MM time I - VI	0.9 – 86.4 ks (15 min-24 h) varied
milling temperature	< 25 °C (vessel inside by Maltoz)
feeding system	standard air-lock DN40-KF
discharging/separation	draingrating Ask-01
average powder yield	90-103 %

Table 2: HKP parameters of Ag-Cu-powder in the Simoloyer

For loading the starting powder for each single test, first the mill that must be in charging/operation position is evacuated to around 10^{-4} hPa and then flooded with Argon. The powder, that has been loaded inside a glove-box into a powder-container, was then transferred by the air-lock into the vessel at the same time when the vacuum was flooded since then the gas flow can even be used for the powder transportation.

After the adjusted MM-time elapsed, the grinding unit is tuned into discharging position and the same air-lock (after cleaning) was used for unloading the powder where this time first the powder container is evacuated via the air-lock. In that way, the gas-flow supported the unloading (a little) and the powder was discharged completely (grinding media remains in vessel).

sampling schedule to investigate flake-formation			
test no.	pow./ball ratio (wt)	sample mass [g]	sample time [min]
01	1:10	0.5	1, 5, 15, 30, 60
02	1:20	1	1, 5, 7, 10, 13, 15, 30
03	1:50	1	1, 3, 5, 7, 10, 15

Table 3: process schedule to investigate flake formation

sampling schedule to investigate SSF			
test no.	pow./ball ratio (wt)	sample mass [g]	sample time [h]
10	1:10	1	5, 20, 24
11	1:20	1	13
12	1:50	1	5

Table 4: process schedule to investigate solid solution formation (SSF)

Figure 3: sampling unit of air-lock DN40-KF

The samples were taken by following the same procedure but instead of the powder container, a sampling unit was used, which is a small glass-tube with a ball valve and an adapter to the proper KF-dimension (figure 3).

Unloading is computerized and automatically operated. In order to increase the powder yield and to decrease the discharging time, Cycle Operation (figure 4) has been applied which means during processing and discharging, the rotational speed of the rotor is changed in a special frequency in the range from here 150-600 rpm which has

been proven to tremendously increase the powder yield of materials that tend to stick and agglomerate under MM to the milling tools and to each other [9-10, 12].

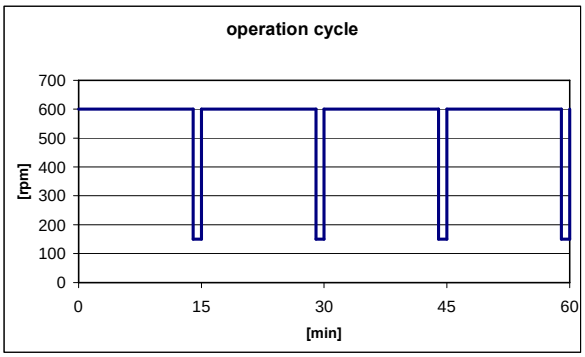

Figure 4: Operation Cycle for MM

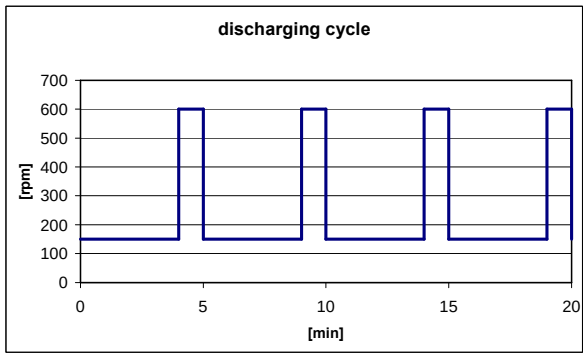

Figure 5: Discharging Cycle after MM

By this method in average complete powder yield could be obtained. Since between the each of the different MM-operations, the system has never been opened and since a little amount of powder always remains in the system e.g. sticking to grinding balls and vessel, the powder yield varied between 90 and 103 % after Discharging-Cycle of 10-20 min at 600/150 rpm (figure 5). Both of the cooling systems (vessel and pre-seal-unit) were constantly operated and the computerized measurement of the inner-vessel surface indicated temperatures lower than 25°C.

2.3 Powder Characterization

The initial and the as milled powders were characterized by SEM, XRD and TEM.
For Scanning Electron Microscopy, we applied a Jeol JSM-6300 and prepared the powder samples on a graphite tape in order to observe morphology and size. The iron-contamination of the powder samples has been investigated by Microanalysis using the same device.For X-ray diffraction we applied a Siemens Diffractometer D 5000 using monochromatic Cu-Kα radiation and determined/estimated the grain size by the Scherrer method and later confirmed by TEM. For Transmission Electron Microscopy we applied a Jeol JSM 2000 FXII and used an ultrasonic bath to de-agglomerate the powder samples and then mounted on copper grids.

3. Results

3.1 SEM and Microanalysis (flake formation)

Figures 6a and 6b show the SEM-micrographs of the starting powders (a) Cu and (b) Ag. Copper presents rounded shape with some porosity and an average particle size of around 5 µm, Silver shows an elongated shape with an average particle size between 1-10 µm.

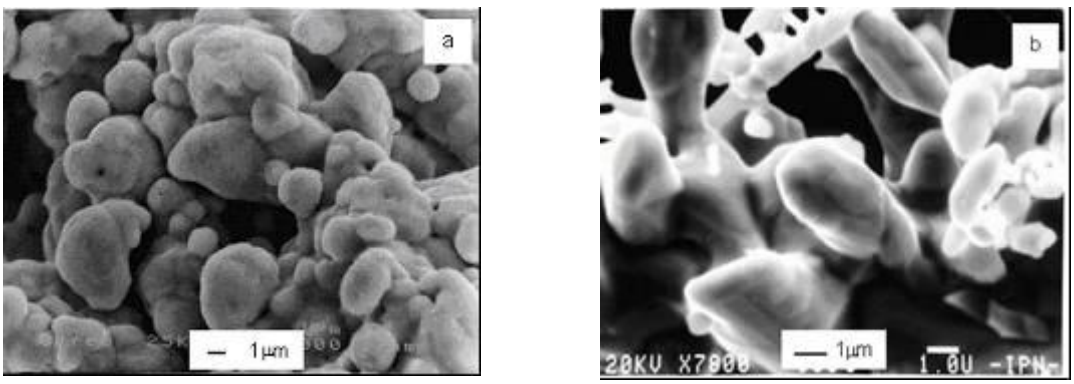

Figure 6: SEM-micrographs of the starting powders (a) Cu and (b) Ag

Figures 7a1/a2 give the SEM-micrographs of the sample taken after 0.06 ks (1 min), figure 7 b1/b2 after 0.3 ks (5 min) and figure 7 c1/c2 after 0.9 ks (15 min). This data refers to test 01 which means the powder/ball weight ratio was 1:10, 1.4 kg of grinding media was in the grinding unit and in total 140 g of powder mixture Ag/Cu was loaded. Figures a2-c2 always show a higher resolution of the corresponding a1-c1 SEM-image.

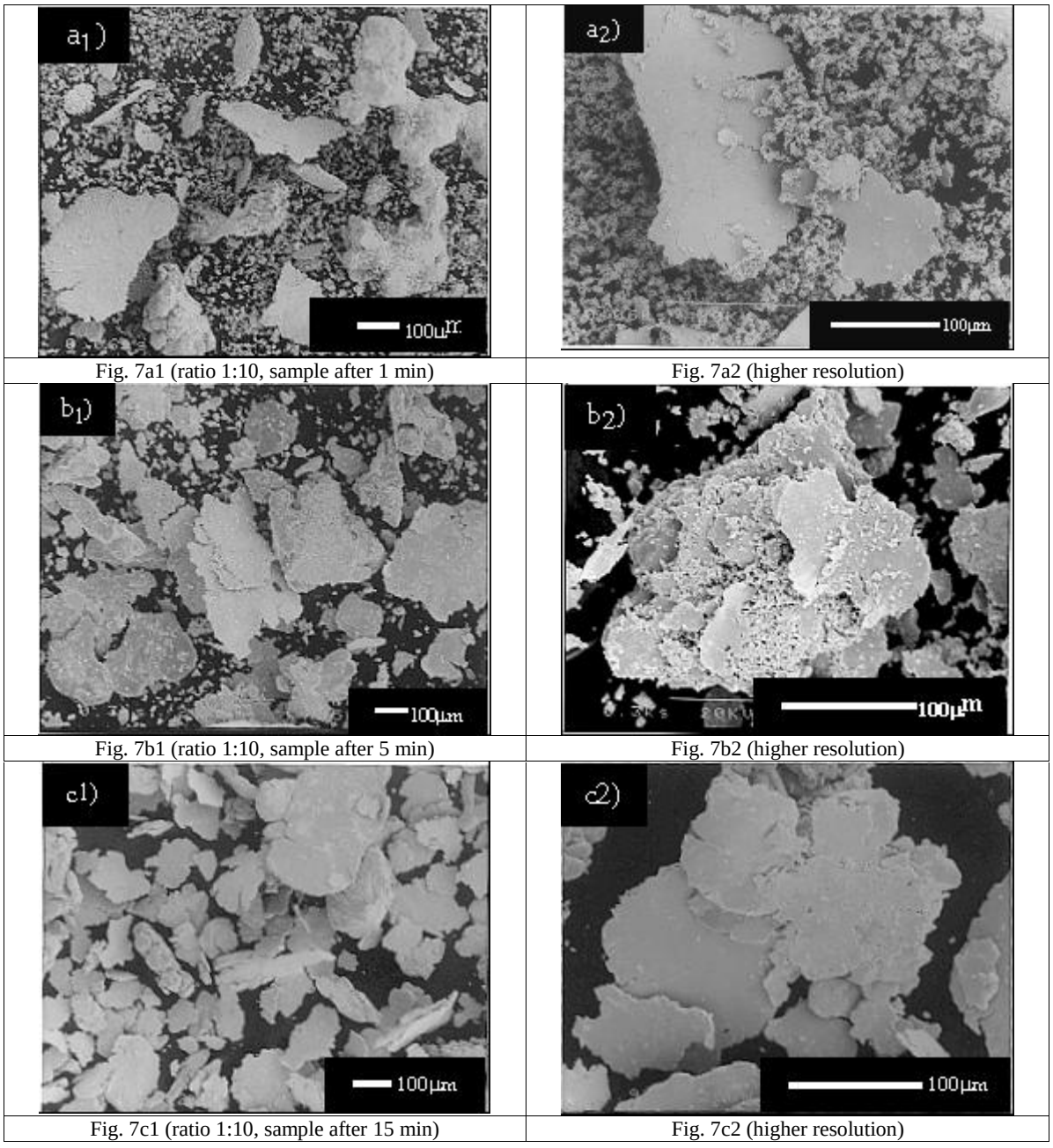

Fig. 7a1 (ratio 1:10, sample after 1 min) | Fig. 7a2 (higher resolution)

Fig. 7b1 (ratio 1:10, sample after 5 min) | Fig. 7b2 (higher resolution)

Fig. 7c1 (ratio 1:10, sample after 15 min) | Fig. 7c2 (higher resolution)

Figure 7a-c: SEM-micrographs of Ag-70Cu powder samples after HKP at a load ratio of 1:10

The given SEM-investigation confirms after just 1 minute of processing time (figures 7a1 and 7a2) already a complete change of morphology of the Ag/Cu-powder. Following the expected evolution, we would describe first the still most present fine powder fraction which also dramatically changed the appearance which can be seen at figure 7a2 at higher resolution. This fraction my be described as loose low dense powder-agglomerates where the primary particle size (PPS) is close to the original size of the starting powders and the secondary particle size (SPS), so the size of the bulks is in the order of 10-50 µm. Then we can see some large and very irregular bulks in the size of 100-200 µm that must have been formed from the lower dense agglomerates and finally a few huge flakes as large as about 200-

350 µm can be observed. Most probably these flakes, that are already quite thin in the order of only a few µm will have been formed by flattening the huge bulks.
So in principle we expect the fine powder to be agglomerated and maybe already slightly cold welded to huge bulks and then those ones are flattened and get into the flaky shape. A basic idea here is, that the kinetic impact does not apply at highest efficiency to fine particles because of the dumping effect of the same. So here we only expect agglomeration. Once we have bigger agglomerates in the process, then the colliding grinding media will compact these very low dense agglomerates quite rapidly and since there is not such significant dumping effect any longer, density will increase and cold-welding will start. At this stage we actually would not assume to much interaction of deformation and fracture since fracture can only start once high dense flakes are available.

After 5 minutes MM, as seen in figure 7b1 and 7b2 respectively, we can clearly see that the procedure we expected before seems to go on. Now we have much less fine fraction, not a significantly higher amount of huge bulks but a very much increased fraction of huge flakes. Additionally it seems, that we see some fractures of former larger flakes and also we see that flakes are agglomerated with other flakes which can be seen very nicely at figure b2 at higher resolution. And most important, here we can see, that particles of the remaining fine fraction are agglomerated to the surface of already compacted flakes. By this, these small particles will be exposed to the kinetic impact of the grinding media and by this very rapidly a kind of multi-layer structure is expected to be built. The size of the flakes is far different in the order of 100-350µm.

After 15 minutes, as seen in figures 7c1 and 7c2, again, we can observe a tremendous change and this time the entire morphology appears different. The originally fine fraction completely disappeared and the large flakes have in comparison to earlier evolution stage a very smooth surface. At higher resolution, in figure 7c2, we can actually determine two different appearances since in the center of the image we see some large flakes where earlier particle borders can be seen which means these flakes most probably have been built up by multi-layer structure. The flakes to be seen on the left do not show this kind of surface and are either less or further in evolution which means cold welding and deformation went on for the first or the second type. The size of the flakes is not that much different in the order of 80-150µm.

In table 5 we try to summarize the above where we estimate the flaky fraction in proportion to the material covered image area and call this 1D. Additionally to the size we very carefully estimated the flake thickness and then conclude to the average aspect or cross-ratio:

SEM-results related to flake-formation at the powder/ball weight ratio of 1:10, estimates				
MM-time [min]	flaky fraction 1D [%]	flake diameter [µm]	flake thickness [µm]	cross-ratio
1	10	200-350	5-10	36.6
5	30	100-350	10-20	15
15	95	80-150	10-40	4.6

Table 5: summary of SEM-results related to flake-formation at the powder/ball weight ratio of 1:10

From the numbers carefully estimated in table 5, we can of course and very clearly see, that the fraction of flakes is increasing with the processing time and that the flakes become smaller and thicker which maybe also explained by an embrittlement of the material by surface hardening due to cold welding effects.
Looking at the cross-ratio, we have to notice, that we have no ductile metal flakes in common sense here since then we would need to obtain cross-ratios in the order of 200 and above. But at the same time we have to take into account that here we have flakes that are built up by smaller and thinner flakes where in conventional flake processing, exactly this is avoided usually by applying a low kinetic process in a drum-ballmill and by adding lubricating PCA's in to the process, often by wet-processing e.g. in alcohol.

Figures 8a1/a2 give the SEM-micrographs of the sample taken after 0.06 ks (1 min), figure 8 b1/b2 after 0.3 ks (5 min) and figure 8 c1/c2 after 0.6 ks (10 min). This data refers to test 02 which means the powder/ball weight ratio was 1:20, 1.5 kg of grinding media was in the grinding unit and in total 75 g of powder mixture Ag/Cu was loaded. Figures a2-c2 always show a higher resolution of the corresponding a1-c1 SEM-image.
Since in case of a higher powder/ball weight ratio, we can expect a higher effect of the kinetic impact on our material since the dumping effect of the same is significantly reduced, we expected flake formation in shorter time and therefore extracted and characterized powder samples after shorter time as 1, 5 and 10 minutes.

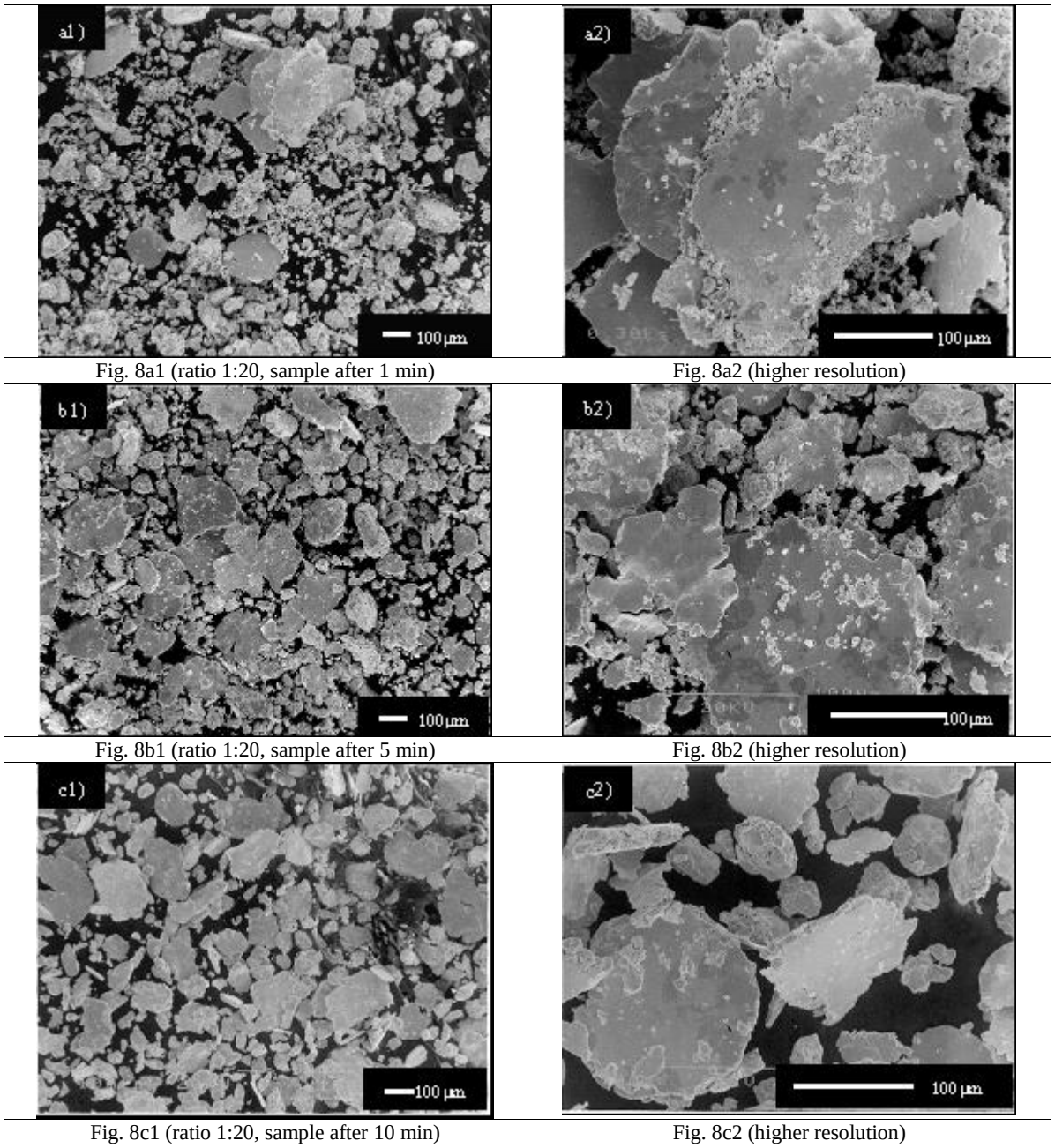

Fig. 8a1 (ratio 1:20, sample after 1 min) | Fig. 8a2 (higher resolution)

Fig. 8b1 (ratio 1:20, sample after 5 min) | Fig. 8b2 (higher resolution)

Fig. 8c1 (ratio 1:20, sample after 10 min) | Fig. 8c2 (higher resolution)

Figure 8a-c: SEM-micrographs of Ag-70Cu powder samples after HKP at a load ratio of 1:20

The given SEM-investigation at the higher powder ball/weight ratio of 1:20 confirms after 1 minute of processing time (figures 8a1 and 8a2) also a complete change of morphology of the Ag/Cu-powder. The evolution is expected similar to what has been described before for the ratio 1:10, however, the appearance we find here, is different from before. We do not see the reported large bulks and it seems, that here the evolution is already further in time development.

The still most present fine powder fraction may still be described as loose low dense powder-agglomerates where the PPS is close to the original size of the starting powders and the SPS, so the size of the bulks is in the order of 10-50 µm. Then we can see some few medium to large sized flakes in the order of 100-200 µm.
In accordance to the expectation given before for the test 01 we expect here agglomeration and cold welding. The remaining fine powder fraction is significantly lower and we can see already flakes with agglomerates of this fraction on the surface.

After 5 minutes MM, as seen in figure 8b1 and 8b2 respectively, the described procedure seems to go on. We find much less fine fraction and an increased fraction of huge flakes and this in the before described multi-layer structure. The size of the flakes is far different in the order of 50-200µm which is significantly smaller than in test 01 after the same processing time.

After 10 minutes, as seen in figures 8c1 and 8c2, the entire morphology appears different. The originally fine fraction completely disappeared, the very large flakes seem to have been broken and we can see a number of small bulks and flaky fractures and some larger flakes. The surface of the flakes got more smooth but they appear to have a relatively higher thickness than after 15 minutes at the ratio 1:10 (figures 7c1 and c2). At higher resolution, in figure 8c2, we can determine large flakes where earlier particle borders can be seen which means these flakes have been built up by multi-layer structure. The size of the flakes is different in the order of 40-150 µm.

Table 6 gives the estimate summary of the above based on the same criteria as given for table 5:

SEM-results related to flake-formation at the powder/ball weight ratio of 1:20, estimates				
MM-time [min]	flaky fraction 1D [%]	flake diameter [µm]	flake thickness [µm]	cross-ratio
1	20	100-200	5-10	20
5	40	50-200	10-20	8.3
10	95	40-150	10-20	6.3

Table 6: summary of SEM-results related to flake-formation at the powder/ball weight ratio of 1:20

From the numbers carefully estimated in table 6, we can again see, that the fraction of flakes is increasing with the processing time, that the flakes become smaller and thicker and that the estimated cross-ratio is again decreasing.

Figures 9a1/a2 give the SEM-micrographs of the sample taken after 0.06 ks (1 min), figure 9 b1/b2 after 0.18 ks (3 min) and figure 9 c1/c2 after 0.3 ks (5 min). This data refers to test 03 which means the powder/ball weight ratio was 1:50, 1.5 kg of grinding media was in the grinding unit and in total 30 g of powder mixture Ag/Cu was loaded. Figures a2-c2 always show a higher resolution of the corresponding a1-c1 SEM-image.

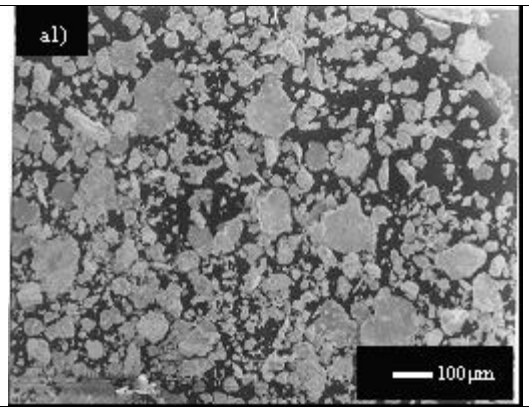

Fig. 9a1 (ratio 1:50, sample after 1 min)

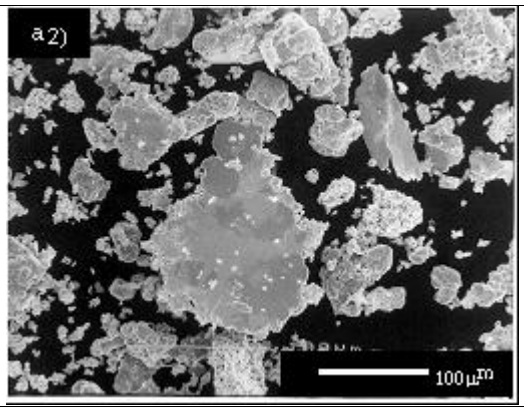

Fig. 9a2 (higher resolution)

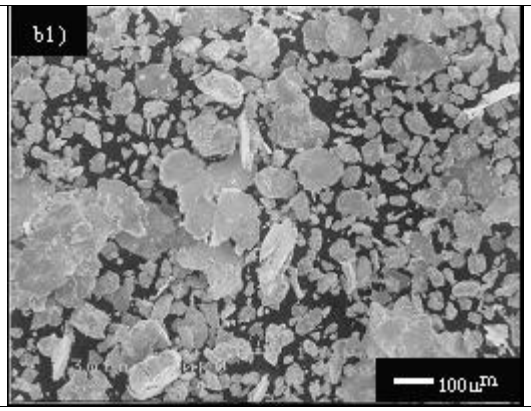

Fig. 9b1 (ratio 1:50, sample after 3 min)

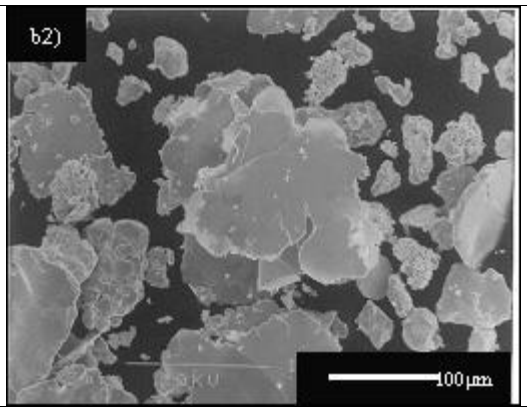

Fig. 9b2 (higher resolution)

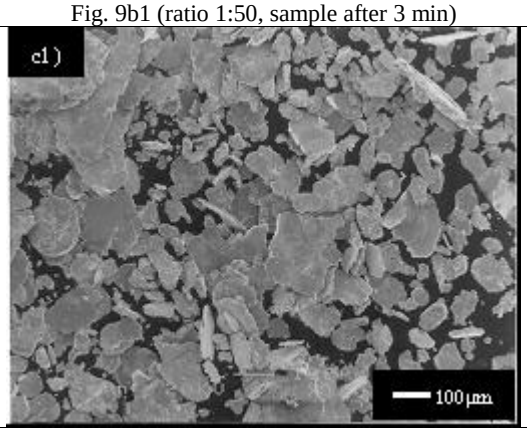

Fig. 9c1 (ratio 1:50, sample after 5 min)

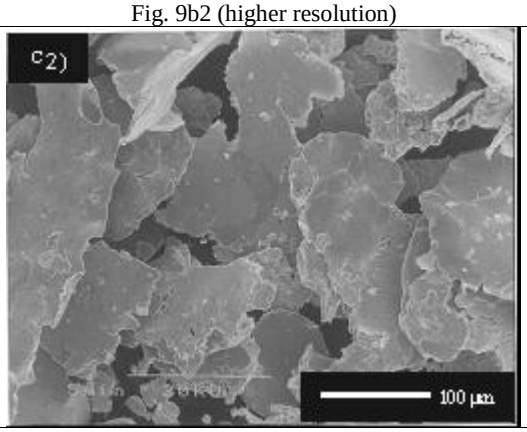

Fig. 9c2 (higher resolution)

Figure 9a-c: SEM-micrographs of Ag-70Cu powder samples after HKP at a load ratio of 1:50

The given SEM-investigation at the higher powder ball/weight ratio of 1:50 confirms after 1 minute of processing time (figures 9a1 and 9a2) a complete change of morphology of the Ag/Cu-powder. The evolution is expected similar to what has been described before for the ratio 1:10 and at ratio 1:20, however, the appearance we find here, is different from before. We can not see the reported large bulks in case of ratio 1:10 and in comparison to the ratio 1:20 the fine powder fraction described as loose low dense powder-agglomerates is almost not present where the expectation is, that it already disappeared. This would mean, that here the evolution is already much further in time development.
For the expected remains of the powder-agglomerates, the PPS is expected to be close to the original size of the starting powders and the SPS, so the size of the bulks is in the order of 10-50 µm. The most present fractions are flakes in the order of 30-150 µm. In accordance to the expectation given before for the test 01 and test 02 we expect here agglomeration and cold welding. The remaining fine powder fraction is almost disappeared and we can see flakes in different stadiums flattened agglomerates and cold welded multi-layer structured flakes with agglomerates of the remains of the fine fraction on the surface.

After 3 minutes MM, as seen in figure 9b1 and 9b2 respectively, the described procedure seems to go on. The fine fraction is completely disappeared and we can only find flakes in both stadiums where the surface becomes smoother and the size increased to the order of 30-250 µm.

After 5 minutes, as seen in figures 9c1 and 9c2, the flakes described as flattened agglomerates completely disappeared and we can only see cold welded multi-layer structured flakes. The size seems to be grown to the order of 50-350 µm.
At higher resolution, in figure 9c2, we can see only a very few number of residues of the originally fine fraction agglomerated on the surface of some of the flakes where in all cases earlier particle borders can be seen which proves the multi-layer structure.
The evolution of flake development seems further that in test 01 after 15 and in test 02 after 10 minutes.

Table 7 gives the estimate summary of the above based on the same criteria as given for tables 5-6:

SEM-results related to flake-formation at the powder/ball weight ratio of 1:50, estimates				
MM-time [min]	flaky fraction 1D [%]	flake diameter [µm]	flake thickness [µm]	cross-ratio
1	50	30-150	no	no
3	95	30-200	10-20	9.3
5	95	50-250	5-15	20

Table 7: summary of SEM-results related to flake-formation at the powder/ball weight ratio of 1:50

From the numbers carefully estimated in table 7, we can again see, that the fraction of flakes is increasing with the processing time. On the contrary to the earlier tests 01 and 02 we cannot determine at the chosen sampling-times, that the flakes become smaller which does probably not mean that we find a different evolution here and will be commented when we directly compare the results (see chapter 4). Thickness and cross-ratio cannot be commented here since we can not draw corresponding conclusions from the SEM-images 9a1 and a2.

The graph in figure 10 gives the results related to tests 01-03 from the Fe-mapping which we achieved by microanalysis investigating at least 10 areas per spot.

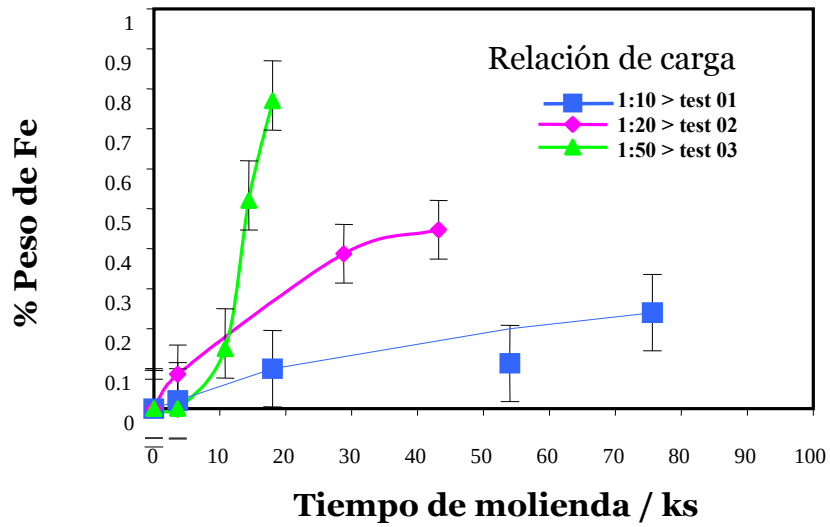

Figure 10: Fe-contamination by microanalysis (min. 10 areas each)

It must be noticed, that the given graph in figure 10 covers the complete measurement not only for the shorter terms up to 15 min (0.90 ks) for the investigation of flake formation but also for longer terms for the investigation of solid solution formation (SSF).

By experience, it is known, that in case of the Simoloyer, almost no contamination is caused by the vessel of the grinding chamber since this is not exposed to high kinetic impact and that only a small fraction (< 5 %) is caused by the rotor which is exposed to high kinetic impact but has a small surface only. The main contaminant is the grinding media (> 95 %) which is exposed to high kinetic impact and exhibits large surface. Since in the tests 01-03, the grinding media load was relatively constant (1400-1500 g), the contamination variation is expected to be caused by different grade of kinetic impact. On the other hand, the powder/ball weight ratio has a direct influence on the kinetic in the system since the powder itself provides a dumping effect against the kinetic impact (acts like liquid).
Next to this, contamination of the grinding media in case of the Ag-Cu-system will then be expected higher, if not all collisions of the grinding media will take place at in-between powder since the hardness of the grinding media is significantly higher than the one of both starting powder materials. In other words, a direct collision of grinding media without powder will cause highest contamination of the same and this means a) with respect to Fe-contamination and b) with respect to kinetic impact that the load-ratio shall not be to high. The results in figure 10 match with the explanation before since we can see that the Fe-contamination increases with the powder/ball weight ratio. The crossing of the curve 1:50 with the curve 1:20 at approximately 3 h (10.8 ks) and the crossing of the curve 1:20 with the curve 1:10 at approximately 50 min (3 ks) are explained with the general measurement range of the mapping by microanalysis and may also depend on the disappearing of the fine powder fraction in early stage up to 10 minutes and on the expected work-hardening on the surface of the formed flakes.

For the here observed flake-formation, the Fe-contamination is always detected below 0.05 %.

In order to conclude a comparison of flake formation (and Fe-contamination) at different powder/ball weight ratios, we determine the flake formation to that point when the fine powder fraction is completely disappeared. This attempt is shown in table 8:

SEM-results including microanalysis in survey			
powder/ball weight ratio	flake formation after		Fe-contamination
	[min]	[ks]	[wt %]
1:10	15	0.90	< 0.05
1:20	10	0.60	< 0.05
1:50	5	0.30	< 0.05

Table 8: results of SEM-micrographs and microanalysis in survey

3.2 XRD (SSF)

The powder characterization by XRD is related to the tests 10-12. These separate tests at same conditions as the previous tests 01-03 were chosen because much longer processing times for the formation of a solid solution in the Ag-Cu-system are expected. Figure 11-13 show the XRD-patterns of the processed powders achieved after MM at various times from 3.6 to 86.4 ks at the different applied powder/ball weight ratio of 1:10, 1:20 and 1:50 respectively:

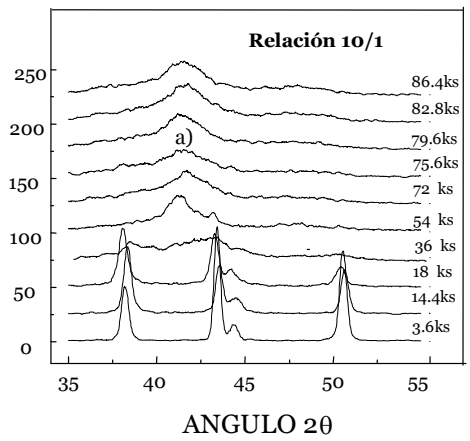

Figure 11: XRD-patterns of processed powders at p/b-wt ratio of 1:10

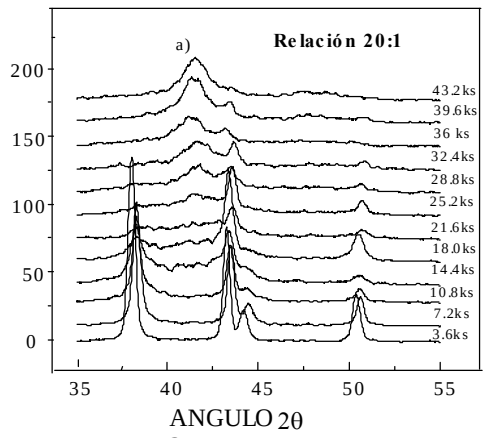

Figure 12: XRD-patterns of processed powders at p/b-wt ratio of 1:20

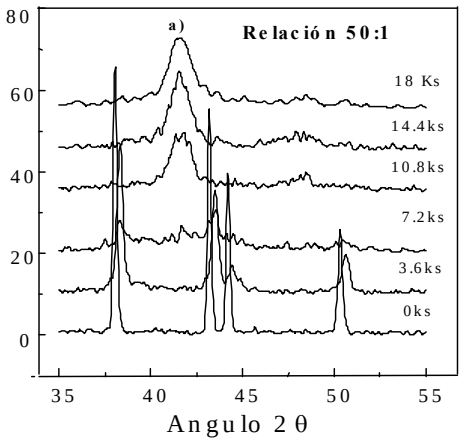

Figure 13: XRD-patterns of processed powders at p/b-wt ratio of 1:50

We determine the solid solution formation (SSF) by the detection of the (111), (200) and (220) planes of the SS. This gives us good data for the beginning of SSF at least.
In figure 11 we see the XRD-patterns which are related to the powder/ball weight ratio of 1:10 and the SSF is detected at 54 ks (ignition) and seems to be completed at 79.2 ks. In figure 12 we see the XRD-patterns which are related to the powder/ball weight ratio of 1:20 and the SSF is detected at 36 ks (ignition) and seems to be completed at 43.2 ks. In figure 13 we see the XRD-patterns which are related to the powder/ball weight ratio of 1:20 and the SSF is detected at 14.4 ks (ignition) and seems to be completed at 18 ks.

3.3 TEM (SSF)

We applied TEM-investigation to check if the SSF detected by XRD is completed. This could be expected e.g in case of test 12 after 14.4/18 ks according to the XRD-data. The TEM-results after 18 ks are given in figure 14a-c, all other investigation can be found in parallel work [15].
From angle measurement we calculated the lattice parameter to 3.769 Å. The grain size determined by the Scherrer-method is given at < 10 nm, the grain size determined by TEM at 5-30 nm.

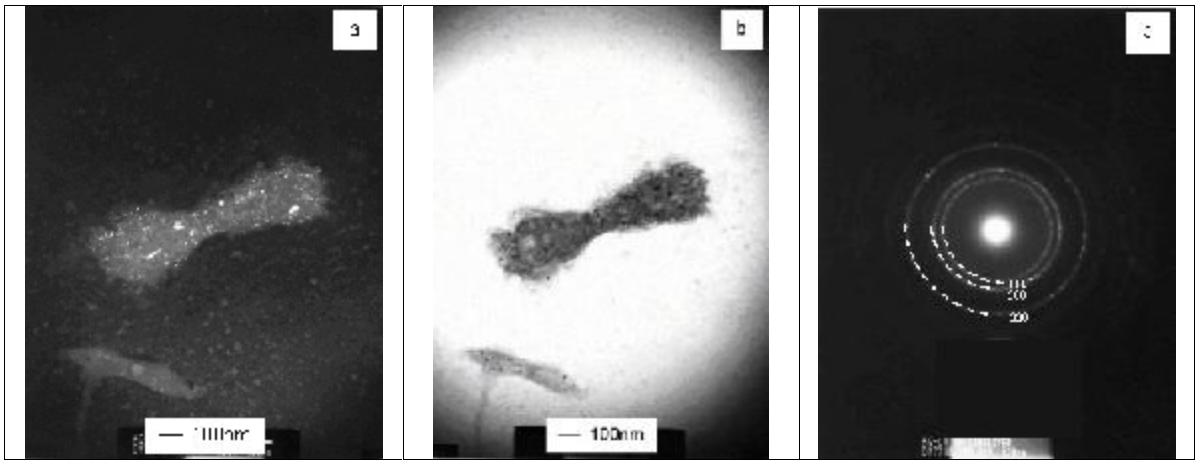

Figure 14: TEM-investigation of the MM powders in the Simoloyer: (a) darkfield micrograph, (b) brightfield micrograph, (c) diffraction pattern after 18.0 ks

The dark- and brightfield micrographs (a, b) show a grain size at around 5-30 nm where we obtained a value of 5 nm by the Scherrer-method. The diffraction pattern (c) shows diffraction rings which are characteristic for the nanometric grains of the new solid solution formed.

4. Relation of Flake-formation, SSF and Fe-contamination

The comparison of the received results by SEM-micrographs and microanalysis, XRD and TEM is given in table 9:

SEM-, XRD- and TEM-results (including microanalysis) in survey						
powder / ball weight ratio	flake formation		Fe-contamination after time a	SSF		Fe-contamination after time b
	starts after	completed after [a]		starts after	completed after [b]	
	[ks]	[ks]	[wt %]	[ks]	[ks]	[wt %]
1:10	0.06	0.90	< 0.05	54	79.2	0.25
1:20	< 0.06	0.60	< 0.05	36	43.2	0.45
1:50	< 0.06	0.30	< 0.05	14.4	18	0.75

Table 9: results of SEM-micrographs and microanalysis, XRD and TEM in survey

The graph in Figure 15 gives the dependency of flake-formation and SSF at different powder/ball weight ratios. The measured data at each of the different ratios was concluded to a curve which shows that the slope of the 2 curves for flake formation and SSF are almost equal which was expected since the driving force for both formations was earlier defined as being dependent on the kinetic impact and the kinetic impact was described to be determined by the powder/ball weight ratio in these experiments.
Figure 16 gives the dependency of SSF and Fe-contamination at different powder/ball weight ratios 1:10, 1:20 and 1:50.
What we see here is, that in case of higher powder/ball weight ratio, the solid solution is completed earlier, but the Fe-contamination is higher even at the shorter time needed for SSF-evolution. For lower ration, time is longer and contamination remains lower.

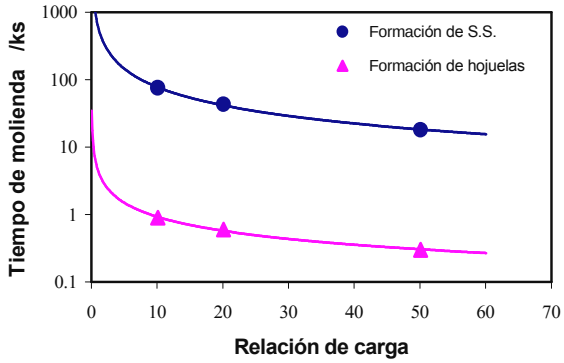

Figure 15: flake-formation and SSF at different powder/ball weight ratios

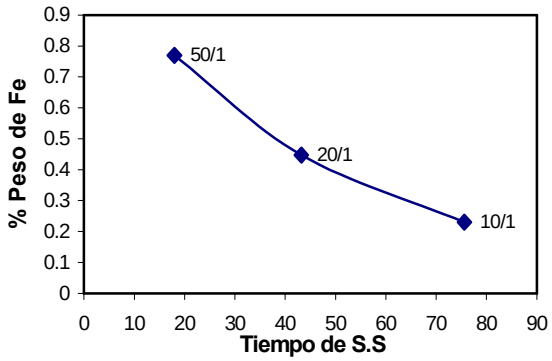

Figure 16: SSF and Fe-contamination at different powder ball weight ratios

5. Conclusions and References

Conclusions

The Ag-70Cu (at%) has been MM in a Simoloyer CM01-2l high energy ball mill at different powder/ball weight ratio and not under high but under medium kinetic.
The flake formation started after a processing time of 0.06 ks and below and was observed to be completed after 0.3, 0.6 and 0.9 ks at load ratios 1:50, 1:20 and 1:10 respectively. The Fe-contamination by the milling tools which means here mostly by the grinding media was detected to be very low at < 0.05 wt % in all cases:

completion of flake formation						
powder / ball weight ratio		flake formation completed		Fe-contamination		comment
[wt %]	factor	[ks]	factor	[wt %]	factor	
1:10	1	0.90	3	< 0.05	(1)	contamination always < 0.05 wt %
1:20	2	0.60	2	< 0.05	(1)	2x higher ratio, 2x shorter time
1:50	5	0.30	1	< 0.05	(1)	5x higher ratio, 3x shorter time

Table 10: completion of flake-formation and comments

From these results we may conclude that the ratio of 1:50 is unnecessarily high for the formation of flakes and may need to be only 1:30 since we can only achieve a 3 times shorter time by the ratio 1:50. This shall be checked by further work and from today's point of view could be explained since a to high ratio will lead to a number of quasi useless collisions where no flake is formed but contamination expected to be increased.

The solid solution formation by MM of Ag-70Cu in the Simoloyer CM01-2l at medium kinetic impact could be obtained at nanometric grain size after18, 43.2 and 79.2 ks at load ratios 1:50, 1:20 and 1:10 respectively. The Fe-contamination did increase with the MM-time from 0.25 to 0.45 to 0.75 wt % and did not reach 1 wt % at any time:

completion of SSF						
powder / ball weight ratio		SSF completed		Fe-contamination		comment
[wt %]	factor	[ks]	factor	[wt %]	factor	
1:10	1	79.2	4.4	0.25	1	contamination always < 1.0 wt %
1:20	2	43.2	2.4	0.45	1.8	2x higher ratio, 2.4x shorter time, 1.8x higher contamination
1:50	5	18	1	0.75	3	5x higher ratio, 4.4x shorter time, 3x higher contamination

Table 11: completion of SSF and comments

From these results we may conclude that the ratio of 1:50 is slightly to high for the SSF and may need to be only 1:44 since we can only achieve a 4.4 times shorter time by the ratio 1:50. This shall be checked by further work and from today's point of view could be explained since a to high ratio will lead to a number of quasi useless collisions where no kinetic impact on Ag-Cu-particles is performed but contamination increases.
What must be pointed out here is, that the contamination is higher for the higher load ratio even at the shorter times. This means if in absolute numbers the contamination shall be reduced, then a lower ratio shall be chosen which is not valid once looking for flake formation only.

In result of this work, we can see that flake formation and SSF do depend both on the powder/ball weight ratio which is a determination of the kinetic in the process. Shifted in processing time, the evolution of both seems to be relatively linear.
The first explanation is of course that for both transformations, kinetic energy impact is determining.
Next to this, the formation of flakes by thin multi-layers seems to favor SSF.
Since in case of SSF, here, Ag-atoms shall be located in the Cu-lattice intersticially or by substitution, this is provided mainly by kinetic impact which means it is of major importance, how this kinetic impact can effect the lattice structure.
E.g. if some grinding media would be thrown into a volume of Ag-Cu-powder, there will be plastic deformation of the volume and there may be plastic deformation of some of the direct hit particles in the front-layer but it is very much unlikely, that this can cause atomic dislocations in the lattice of the materials. This means the dumping effect of the powder plays the same important role for SSF as well as for flake formation. If we now take into account, that ductile metal flakes based on Ag and Cu and others can easily be produced by HKP in short times at flake thickness of 0.5 µm and below [6-8], and that these flakes can be built up by a number of approximately 50 theoretical inter-layers according to the starting particle size [4], then we would end up with a theoretical thickness in 10 nm range.
If we apply this to a powder mixture and use the principle of MA and produce a kind of sandwich, then we probably end up with very short diffusion ways inside this structure and this could explain why multi-layer flake formation favors SSF and it will be very interesting to find dependencies for this in the ongoing work where one of the next steps will be the application of HKP at 3-4 times higher relative velocities of the grinding media.

References

[1] K. Uenishi, K.F. Kobayashi, K.N. Ishihara, P.H. Shingu: "Formation of a supersatured solid solution in Ag-Cu systems by mechanical alloying", Mat. Sci. & Eng. A 134 (1991) pp 1342-1345

[2] R. Esquivel-González, Ph D. Tesis, Compactacion dinamica de materiales nanocristalinos obtenidos por aleación mecanica", ESIQIE-IPN, México (2001)

[3] R. Esquivel G., I. Vernet P., C. Renero y D. Jaramillo V.:Dynamic compaction of nanostructured alloys obtained by mechanical alloying, Journal of Materials of Materials Processing Technology, Thermec 2000 - Processing & Manufacturing of Advanced Materials, TMS, Elsevier Science, (2001)

[4] H. Zoz: HEM/MA/RM - Devices in use, 3rd Intern. Symp. of THE SCHOOL OF CHEMICAL ENGINEERING, IPN, Mexico City, May 27-29, 1998

[5] A. Bose, K. Ameyama, S. Diaz de la Torre, D. Jaramillo V., D. Madang, H. Zoz, Zoz GmbH (Germany & USA), Materials Processing Inc. (USA), Ritsumeikan University, (Japan), CIMAV S.C., ESQIE, (Mexico), F.W. Winter Inc. & Comp. (USA): Review of Applications and Materials processed by Rotating Horizontal High Energy Milling: 2002 World Congress on Powder Metallurgy & Particulate Materials, proceedings (2002)

[6] H. Zoz, D. Ernst, T. Mizutani, H. Okouchi, Simoloyer CM100s, semi-continuously Mechanical Alloying in a production scale using Cycle Operation-Part I, Metall Vol. 51, 10/97, pp. 568-572, 1997

[7] H. Zoz, D. Ernst: Simoloyer CM100s, semi-continuously Mechanical Alloying in a production scale using Cycle Operation-Part II, Metall Vol. 51, 09/98, pp. 521-527, 1998

[8] H. Zoz, H. Ren, H. U. Benz: Ductile Metal Flakes based on [Au], [Ag], [Cu], [Ti], [Al], [Ni] and [Fe] by High Energy Milling - part I, PM2Tech1999 MPIF, Vancouver, (1999) proceedings

[9] H. Zoz, D. Ernst, H. Weiss, M. Magini, C. Powell, C. Suryanarayana, F.H. Froes, Mechanical Alloying of Ti-24Al-11Nb (at%) using the Simoloyer Metall Vol. 50, 09/96, pp. 575-579, 1996

[10] H. Zoz, D. Ernst, I. S. Ahn, W.H. Kwon: Mechanical Alloying of Ti-Ni-based Materials using the Simoloyer, TMS Annual Meeting 1997, eds. C.M. Ward-Close, F.H. Froes, S.S. Cho, D.J. Chellman: Synthesis/Processing of lightweight Metallic Materials, proceedings (1997)

[11] J.Y. Chung, J. Kim and Y.D. Kim: Formation of Nanocrystalline Fe-Co Powders Produced by Mechanical Alloying, Dept. of Metallurgy and Materials Science, Hanyang University, Ansan, Korea, 1999

[12] H. Zoz, H. Ren, N. Späth: Improved Ag-SnO2 Electrical Contact Material Produced by Mechanical Alloying, Metall Vol. 53, 07-08/99, pp. 423-428, 1999

[13] G. Kaupp, M. R. Naimi-Jamal, H. Ren and H. Zoz : Environmentally Protecting Reactive Milling, CHEMIE TECHNIK, 31, vol. 6 (2002) p 58-60

[14] H. Zoz, H.U.Benz, K. Hüttebräucker, L. Furken, H. Ren: Stellite bearings for liquid Zn-/Al-Systems with advanced chemical and physical properties by Mechanical Alloying and Standard-PM-Route, Part I, Metall Vol. 54, 11/2000, pp. 650-659, 2000

[15] H. Zoz, I. Vernet and D. Jaramillo V.: Comparative routes of solid-solution-formation by Mechanical Milling of Ag-70Cu (at%), proceedings of PM2TEC'2003, MPIF (2003)